

Quantum Monte Carlo study of a bilayer $U(2) \times U(2)$ symmetric Hubbard model

Yosef Caplan¹ and Dror Orgad¹

¹*Racah Institute of Physics, The Hebrew University, Jerusalem 91904, Israel*

(Dated: October 26, 2023)

We carry out a sign-problem-free quantum Monte Carlo calculation of a bilayer model with a repulsive intra-layer Hubbard interaction and a ferromagnetic inter-layer interaction. The latter breaks the global $SU(2)$ spin rotational symmetry but preserves a $U(2) \times U(2)$ invariance under mixing of same-spin electrons between layers. We show that despite the difference in symmetry, the bilayer model exhibits the same qualitative features found in the single-layer Hubbard model. These include stripe phases, whose nature is sensitive to the presence of next-nearest-neighbor hopping, a maximum in the Knight shift that moves to lower temperatures with increasing hole doping, and lack of evidence for intra-layer d -wave superconductivity. Instead, we find a superconducting phase, coexisting with stripes, whose critical temperature traces a dome as a function of doping and is due to inter-layer spin-polarized pairing that is induced by the ferromagnetic interaction.

I. INTRODUCTION

Establishing the properties of strongly interacting models, especially in dimensions larger than one, is a difficult problem. A canonical example is the two-dimensional fermionic Hubbard model [1], whose apparent simplicity and widely believed relevance to the high-temperature superconductors have motivated an enormous amount of work over the past six decades. Still, apart from the half-filled system with $n = 1$ electrons per site [2], the weakly interacting limit $U/t \rightarrow 0$, where U and t are respectively the on-site repulsion and intersite hopping [3], and the Nagaoka limit $U/t \rightarrow \infty$ with a single doped hole [4], not much is known with theoretical confidence. Particularly challenging is the intermediate range $U \sim t$, where obtaining a faithful map of the model's behavior depends on numerical calculations.

Currently, the leading technique to study this regime, both in terms of its reliability and ability to handle relatively large systems, is the density matrix renormalization group (DMRG). To date, DMRG has been used to study Hubbard cylinders with up to six legs [5–14], where typically $U/t = 8 - 12$ and $n = 0.875$. The consequences of including next-nearest-neighbor hopping t' were also addressed [9–11, 13, 14]. More numerous are DMRG studies of the t - J model - the large U/t descendent of the Hubbard model, on cylinders with up to eight legs [11, 15–23]. In most cases the calculations were carried out for $J/t = 1/3$, which would correspond to $U/t = 12$ if the mapping to the Hubbard model holds down to this range of interaction strengths, and for hole densities of up to $1/8$. Several studies included t' -hopping, which at times was also accompanied by a J' term [18, 20, 21].

The findings of these studies may be roughly summarised as follows: (i) The vicinity of $t' = 0$ is characterized by charge-density wave (CDW) modulations in the form of filled stripes with one hole per unit length domain wall [7, 8, 11, 12, 21] (nearly half-filled stripes or with $2/3$ filling were also observed [6, 14, 19], and the various types are almost degenerate [8]). They are accompanied by short-ranged spin-density wave (SDW) modulations with

twice the period [11, 19] and by exponentially decaying d -wave superconducting (d -SC) correlations [11, 12] (see, however, Ref. [19]). (ii) The presence of $t' < 0$ causes the stripes to become half-filled [10, 11, 22] or exhibit an intermediate filling between 0.5 and 1 [13]. On four-leg cylinders both the CDW and the d -SC correlations decay as power-laws, but the former dominate. There are conflicting results on wider systems. While only short-range d -SC correlations have been found on a six-leg cylinder [14], non-zero d -SC order was also reported [13]. Regardless, the SDW correlations are still modulated with twice the CDW period and decay exponentially. (iii) For $t' > 0$ and larger than a small threshold the system enters a phase with no stripes and robust power-law d -SC correlations [21–23]. Increasing t' further makes partially-filled stripes reappear. The power-law superconducting correlations decay somewhat faster than the CDW correlations in Hubbard cylinders, while the situation is reversed for the t - J model [11, 14, 21]. In both cases the spin correlations decay exponentially.

Notwithstanding its advantages, DMRG is largely limited to ladder geometries as it involves a computational cost that grows exponentially with the ladder width. Furthermore, it provides information about the ground state, and using it to extract dynamical or finite-temperature information is still in an early stage. Hence, it is desirable to augment DMRG by another method that allows to probe more two-dimensional geometries away from the strict zero-temperature limit. To this end, the determinant quantum Monte Carlo (DQMC) technique appears as the method of choice. Like DMRG it is also unbiased and, in principle, numerically exact. However, away from half filling it is plagued by the sign problem that incurs a prohibitive computational cost as one attempts to explore temperatures much smaller than the bandwidth. Nevertheless, several "brute force" unconstrained DQMC studies [24–27] were able to probe the model down to temperatures of about $T \approx 0.2t$. Their findings show that even at these relatively high temperatures the Hubbard model exhibits ubiquitous and robust stripy correlations, in agreement with the DMRG results. At the same time, no signs of superconductivity were detected.

arXiv:2304.13083v2 [cond-mat.str-el] 25 Oct 2023

Here, we pursue a complementary approach where we use DQMC to study a model that is free of the sign problem, as a computational proxy to the two-dimensional Hubbard model. Specifically, we revisit a bilayer model that was originally introduced by Assaad et al. [28], describing two Hubbard layers that are further coupled by a ferromagnetic interaction between neighboring sites belonging to different layers. While Ref. [28] considered only ground-state stripes correlations for few doping levels and $t' = 0$, we have calculated various charge, spin and superconducting finite-temperature correlation functions over a wide doping range and included the effects of next-nearest-neighbor hopping. Our goal is to contrast the behavior of the bilayer model with the available data on the single-layer Hubbard model in order to establish the level at which the former may be used to glean insights about the latter. This is not a priori clear since the ferromagnetic inter-layer coupling breaks the global $SU(2)$ spin rotation symmetry of the Hubbard model. Concomitantly, it leaves intact a $U(2) \times U(2)$ symmetry, where each $U(2)$ transformation mixes same-spin electrons between the two layers.

Our findings show strong similarities between the electronic signatures of the two models. In particular, the four-leg bilayer sustains spin and charge stripe phases whose dependence on t' and electronic density follows closely that of stripes in the corresponding Hubbard system, as outlined above. The overall trends persist also in the square systems that we have investigated. When $t' = 0$ we find filled charge stripes and spin stripes whose correlation length is larger than the accessible system sizes up to a hole-doping level of about 0.25, from where it steadily decreases. For $t' = -0.25t$, stripes exist over the same doping range but the charge stripes host only 4/5-2/3 holes per unit length of the domain wall, in close resemblance to a recent DMRG study of a six-leg Hubbard cylinder [14]. For $t' = 0.25t$, the square systems exhibit fractionally filled stripes and only above a minimal hole concentration that resides near 1/8. However, we can not rule out their existence at lower doping levels in the thermodynamic limit.

We have looked for signatures of intra-layer d -wave superconductivity by calculating the corresponding susceptibility and vertex function. Our findings for $t' = -0.25t$ and temperatures above $T = 0.2t$ conform with a DQMC study of the Hubbard model under similar conditions [26], which did not provide any evidence for a d -SC instability. Extending the search down to $T = 0.05t$ did not change this conclusion, nor did changing the sign of t' . Despite the fact that the largest values of both the susceptibility and the vertex function were obtained for $t' = 0.25t$ and below 0.2 hole doping, neither show signs of the finite size scaling expected from the onset of d -SC order. In contrast, we did find a sharp rise in the superconducting stiffness at low temperatures to values above the threshold for a Berezinskii-Kosterlitz-Thouless (BKT) transition. We provide evidence that the resulting superconducting phase coexists with stripes and is

due to inter-layer spin-polarized pairing induced by the ferromagnetic interaction. Finally, the uniform spin susceptibility (Knight shift) peaks at a temperature T^* that decreases with increasing doping, as previously found for the Hubbard model [26]. Our ability to probe the bilayer model down to much lower temperatures allows us to detect the leveling off of T^* above 0.3 hole doping.

II. MODEL AND METHODS

To ensure that a fermionic Hamiltonian is free of the sign problem it is sufficient that its kinetic part and its Hubbard-Stratonovich-decoupled interaction commute with some antiunitary operator [29]. A special case is when the fermionic determinant factorizes into two identical real copies, thus guaranteeing its positivity. Pursuing this route, Assaad et al. [28] considered the following bilayer Hamiltonian on a square lattice, which we also study

$$H = - \sum_{l=1,2} \sum_{\sigma=\uparrow,\downarrow} \left(\sum_{i,j} t_{ij} c_{li\sigma}^\dagger c_{lj\sigma} + \mu \sum_i c_{li\sigma}^\dagger c_{li\sigma} \right) - \frac{U}{4} \sum_i (n_{1i\uparrow} - n_{1i\downarrow} + n_{2i\uparrow} - n_{2i\downarrow})^2. \quad (1)$$

Here, l is the layer index, μ is the chemical potential and $n_{li\sigma} = c_{li\sigma}^\dagger c_{li\sigma}$. The hopping amplitudes take the value t between neighboring sites within a layer, and t' between next-nearest neighbors on the same layer. Throughout the paper we use a unit lattice constant and set $t = 1$, which serve as the basic length and energy scales. The interaction is also expressible as $-(U/4) \sum_{li\sigma} n_{li\sigma} + (U/2) \sum_{li} n_{li\uparrow} n_{li\downarrow} - 2U \sum_i S_{1i}^z S_{2i}^z$, where $S_{li}^z = (n_{li\uparrow} - n_{li\downarrow})/2$. Hence, up to a shift of the chemical potential it amounts to local Hubbard repulsion (assuming $U > 0$) on each layer and a ferromagnetic coupling between neighboring sites on different layers. Note that the latter acts to penalize double occupancy on either layers and thus adds to the effective Hubbard repulsion. More importantly, while the interaction is invariant under $U(2) \times U(2)$ transformations acting separately on the two subspaces of same-spin electrons, it breaks the global spin rotation symmetry and introduces effective attraction between the layers.

The particle-hole transformation, $c_{li\sigma} \rightarrow (-1)^i c_{li\sigma}^\dagger$, where the factor $(-1)^i$ equals -1 on one sublattice and 1 on the other, leaves the Hamiltonian invariant with the exception that $t' \rightarrow -t'$. It also changes the average site occupation according to $\langle n \rangle \rightarrow 2 - \langle n \rangle$. Hence, we concentrate on the hole-doped regime $\delta = 1 - \langle n \rangle > 0$, and rely on the relation between the expectation values of observables $\langle \mathcal{O} \rangle(t', \delta) = \langle \mathcal{O} \rangle(-t', -\delta)$ to deduce the behavior in the electron-doped regime from the hole-doped counterparts.

In order to use the DQMC method we decouple the interaction term in the Hamiltonian via a discrete

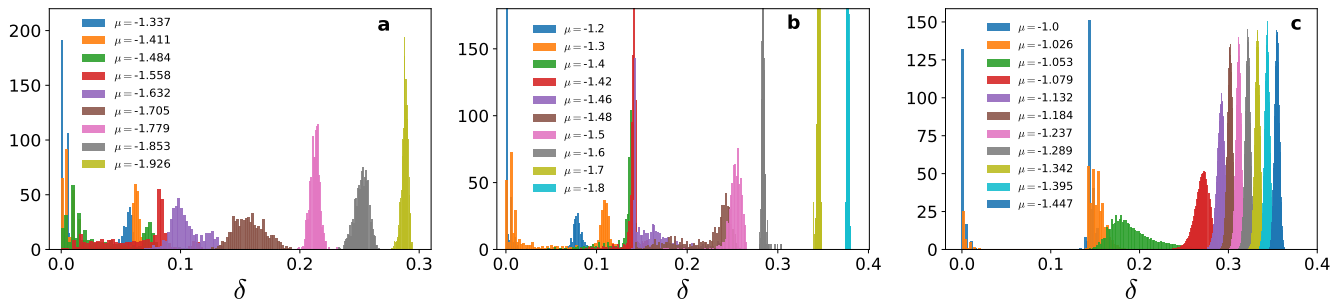


FIG. 1. Histogram of the hole concentration δ obtained from Monte Carlo sampling of a 14×14 square bilayer with (a) $t' = -0.25$, (b) $t' = 0$, and (c) $t' = 0.25$, for various values of the chemical potential μ at a temperature $T = 0.05$.

Hubbard-Stratonovich transformation that involves two Ising-like fields taking values $\pm\psi_{1,2}$. They are accompanied by coefficients a_m [30], which are chosen to ensure the validity of

$$e^{\Delta\tau U \tilde{n}^2} = \frac{1}{4} \sum_{m=1,2} \sum_{\lambda=\pm 1} a_m e^{\sqrt{\Delta\tau U} \lambda \psi_m \tilde{n}} + O[(\Delta\tau)^4], \quad (2)$$

to order $(\Delta\tau)^4$. Here, $\tilde{n} = n_{1\uparrow} - n_{1\downarrow} + n_{2\uparrow} - n_{2\downarrow} = 0, \pm 1, \pm 2$, $\psi_{1,2} = \sqrt{2(3 \mp \sqrt{6})}$ and $a_{1,2} = 1 \pm \sqrt{2/3}$. All of our DQMC simulations were conducted for $U = 4$ and inverse temperatures extending up to $\beta = 20$. For these parameters we used a Trotter step $\Delta\tau = 0.1$, see Ref. [31]. In the following we present our results, obtained by averaging over 40,000-70,000 sweeps, for systems with periodic boundary conditions and sizes of up to 20×20 .

III. RESULTS

A. Phase separation

We begin by mapping the density as a function of the chemical potential with attention to the question of phase separation [31]. The existence of phase separation in the Hubbard model has been controversial. An early DQMC study [32] found no evidence for it when $t' = 0$, while subsequent studies using the dynamical and variational cluster approximations [33, 34] reported its presence for both $t' > 0$ and $t' = 0$. To determine the presence or absence of phase separation in the model studied here, we fix the chemical potential and follow the distribution of the hole concentration δ throughout the Monte Carlo sampling. A bimodal distribution of δ in the thermodynamic limit serves as an indicator for phase separation.

Our results for square $L \times L$ bilayers exhibit a bimodal distribution at low hole doping levels, as depicted in Fig. 1. Specifically, the data in the apparent phase separated regime comprise two peaks, one at half filling ($\delta = 0$) and another that is distributed around an average δ^* . However, when we fix the average hole concentration δ and increase the system size we find that δ^* approaches δ and

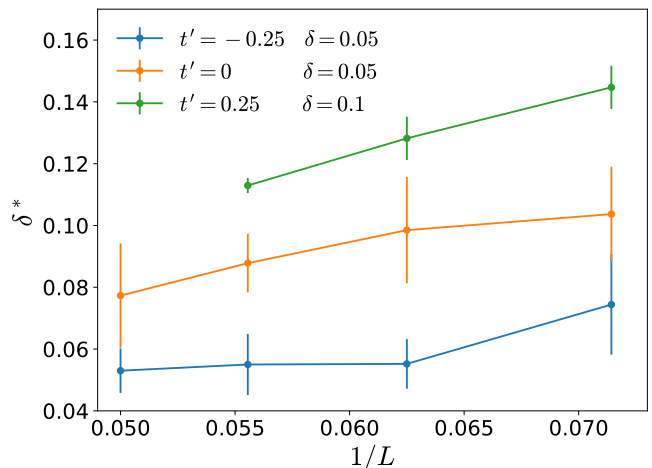


FIG. 2. The size dependence of δ^* in representative systems with fixed average hole concentration δ . The error bars depict the standard deviation of the distribution of hole concentrations that comprise the δ^* peak. For the $L = 20$, $t' = 0.25$ system we find that all Monte Carlo configurations exhibit the same hole concentration $\delta = 0.1$.

that the δ^* peak increases at the expense of the peak at $\delta = 0$. This behavior, shown in Fig. 2 for representative systems with up to $L = 20$, indicates that there is no phase separation in the thermodynamic limit. In particular, the $t' = 0.25$, $\delta = 0.1$ system exhibits $\delta^* = 2/L$ in the range $L = 14 - 18$ (associated with a configuration of two filled charge stripes, as discussed below), whereas already at $L = 20$ we find a single peak at $\delta = 0.1$ with no additional component at half filling. The $t' = 0$ and $t' = -0.25$ systems continue to exhibit bimodal distributions up to $L = 20$, but extrapolating the data suggests that $\delta^* \rightarrow \delta$ upon further increase of the system size.

B. Stripe phases

We have already alluded to the ample numerical evidence for the existence of robust charge and spin stripe

phases in the Hubbard model, especially for $t' \leq 0$. In order to look for similar phases in the bilayer model we have calculated the charge and spin structure factors

$$S_{c,s}(\mathbf{q}) = \frac{1}{2} \sum_{l,i} e^{-i\mathbf{q}\cdot\mathbf{r}_i} \langle\langle n_{c,s}(l, \mathbf{r}_i) n_{c,s}(l, \mathbf{0}) \rangle\rangle, \quad (3)$$

with $n_{c,s}(l, \mathbf{r}_i) = n_{li\uparrow} \pm n_{li\downarrow}$. Henceforth, double angle brackets denote connected correlation functions, i.e., $\langle\langle AB \rangle\rangle = \langle AB \rangle - \langle A \rangle \langle B \rangle$. We have found that over a wide range of parameters S_s exhibits a peak at an ordering wavevector $\mathbf{Q}_s = 2\pi(0.5 - \epsilon_s, 0.5)$ which is typically accompanied by a peak of S_c at $\mathbf{Q}_c = 2\pi(\epsilon_c, 0)$. For square systems we have observed similar features also along the y direction due to rotated configurations of unidirectional stripes. Representative examples are shown in Fig. 3. Peaks at the same momenta also occur in the charge and spin susceptibilities

$$\chi_{c,s}(\mathbf{q}) = \frac{1}{2} \int_0^\beta d\tau \sum_{l,i} e^{-i\mathbf{q}\cdot\mathbf{r}_i} \langle\langle n_{c,s}(l, \mathbf{r}_i, \tau) n_{c,s}(l, \mathbf{0}, 0) \rangle\rangle. \quad (4)$$

Because the $SU(2)$ spin rotation symmetry is explicitly broken by the inter-layer interaction, the spin structure factor and the spin susceptibility differ between the z and x - y directions. We show results for their z -component, defined by Eqs. (3) and (4), for which the peaks are clearly visible. Whenever peaks occur in the S_z spin susceptibility they are also present at approximately the same \mathbf{Q}_s in the susceptibility of the transverse spin components [31]. Nevertheless, whereas the height of the former decreases by more than two orders of magnitude as one moves from half filling to $\delta = 0.3$, the latter are essentially doping-independent and become comparable to their z -counterparts only at high doping levels. We do not find peaks in the transverse spin structure factor.

In order to establish contact between the bilayer model and the Hubbard model, we computed the structure factors of a quasi-one-dimensional periodic bilayer of size 28×4 . Fig. 4a depicts the positions of the peaks in S_s and S_c as a function of δ . For $t' = 0$ we observe sharp spin peaks that follow $\epsilon_s \simeq \delta/2$ within a range of doping levels that extends from 0.08 to about 0.3. Over a considerable portion of this range they are accompanied by charge peaks at $\epsilon_c \simeq \delta$. These signatures are similar to the findings of DMRG [9–11] and DQMC studies [25, 26] of a Hubbard system with the same geometry, and correspond to charge stripes that host one hole per unit length and which serve as π -phase shift domain walls for the antiferromagnetic order. We attribute the absence of stripes at small δ to finite size effects, as one can not embed more than a single stripe within the system while preserving the relation $\epsilon_c = \delta$. Instead, we observe in this regime alternations of the DQMC configurations between a half filled phase and a phase with $\delta = 1/L_x$, which may be associated with a single charge stripe.

The four-leg bilayer model and the corresponding Hubbard system continue to exhibit similar stripy charge and

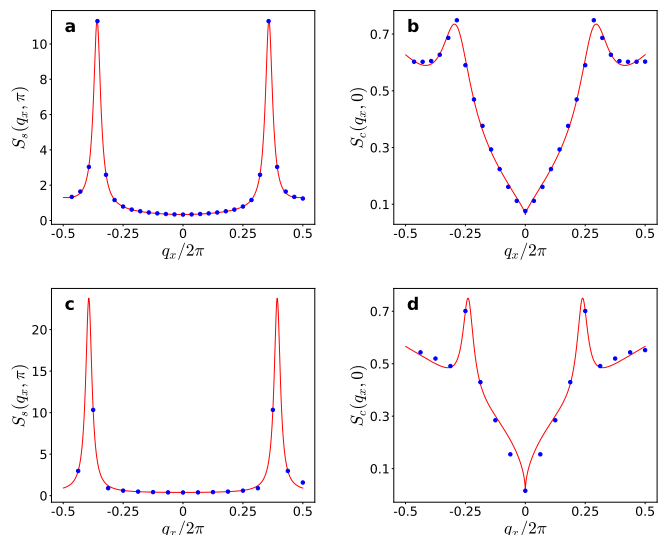


FIG. 3. (a) The spin structure factor $S_s(q_x, \pi)$ and (b) The charge structure factor $S_c(q_x, 0)$ as a function of q_x for a 28×4 periodic system with $t' = -0.25$, $\delta = 0.163$ and $\beta = 10$. The lines are a fit to a double Lorentzian with an added background [35]. The peaks occur at $\epsilon_s = 0.14$ and $\epsilon_c = 0.29$, respectively, and stay put upon lowering the temperature. (c,d) The same quantities for a 16×16 system with the same parameters at $\beta = 20$. The peaks shift from their positions in the cylindrical system to $\epsilon_s = 0.11$ and $\epsilon_c = 0.24$.

spin correlations also when next-nearest neighbor hopping is included. For $t' = -0.25$ and below $\delta = 0.15$ we observe $\epsilon_c \simeq 2\delta$, which indicates that the charge stripes are half filled, as found for the Hubbard cylinder [9]. However, the density of holes on the stripes increases when $0.15 < \delta < 0.3$. In both doping ranges the period of the spin modulations is twice that of the charge density. Here again, we associate the fact that we do not observe stripes at small δ with finite size effects. In contrast, the absence of stripes below $\delta = 0.18$ for $t' = 0.25$ seems to be a true property of the thermodynamic limit of the model, at least in the temperature range that we have considered. This is consistent with the DQMC results for the Hubbard system [25]. We note that at doping levels above $\delta = 0.3$ and for all values of t' , the model exhibits a phase with short-ranged stripe correlations that are accompanied by a change in the dependence of ϵ_s on δ , see Fig. 4a. This range of parameters has not been investigated in the context of the Hubbard cylinder and it would be interesting to close this gap in order to see if the similarities between the models continue to hold true for high doping levels.

Having mapped out the behavior of the quasi-one-dimensional system we proceed to discuss the stripe characteristics of more two-dimensional geometries, which are not amenable to DMRG calculations. Accordingly, we have computed S_s and S_c of $L \times L$ periodic bilayers, with $L = 12 - 20$. The results for $t' = 0$, which are depicted in Fig. 4b, show the same linear doping de-

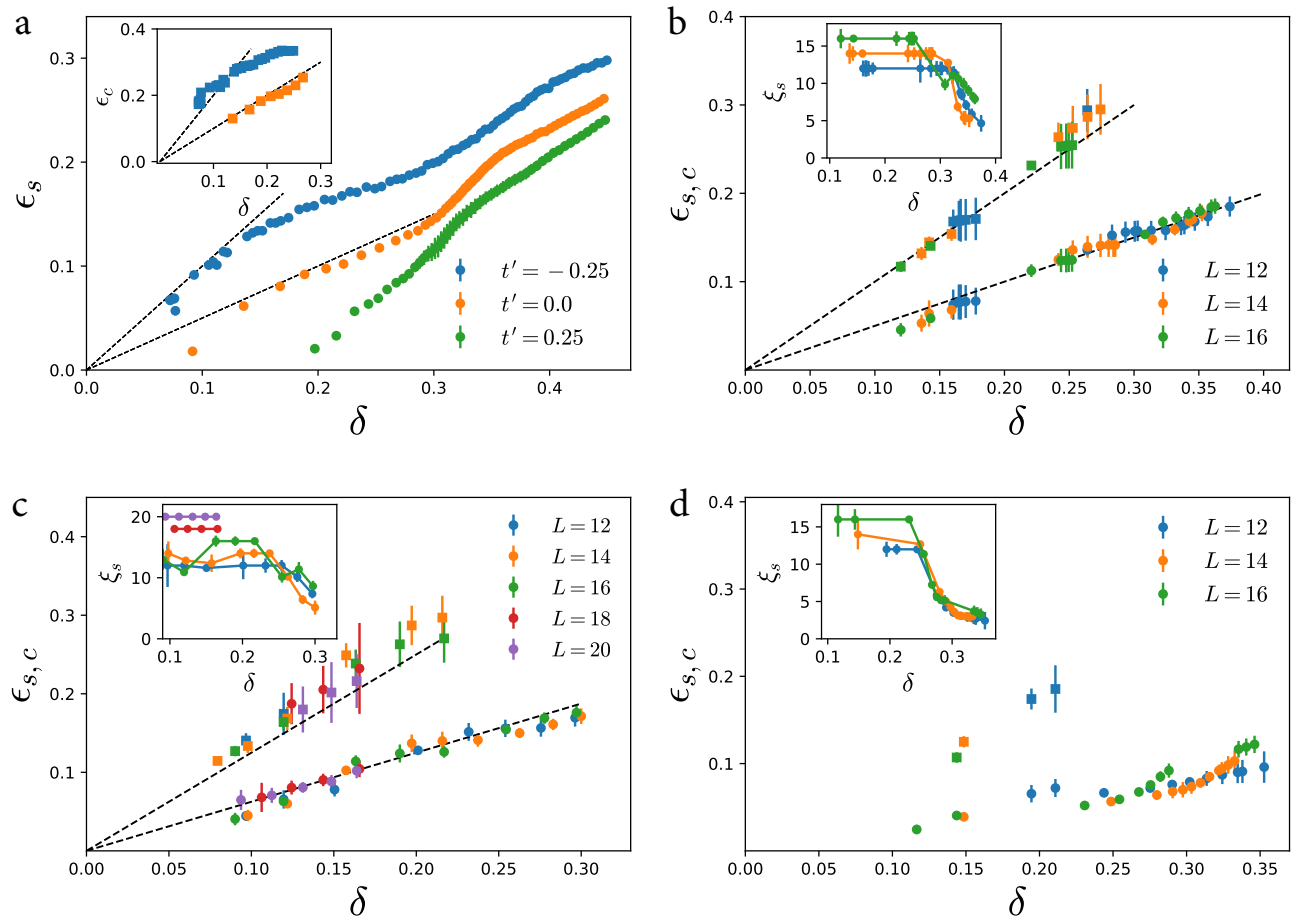


FIG. 4. (a) The position of the peak in S_s for a 28×4 periodic bilayer as a function of hole doping at $\beta = 10$. The dashed lines correspond to $\epsilon_s = \delta/2$ and $\epsilon_s = \delta$. The inset depicts the associated peak position in S_c , where here the dashed lines trace $\epsilon_c = \delta$ and $\epsilon_c = 2\delta$. (b) The position of the peak in S_s (circles) and in S_c (squares) for $t' = 0$ periodic square systems as a function of hole doping at $\beta = 20$. The dashed lines correspond to $\epsilon_s = \delta/2$ and $\epsilon_c = \delta$. The inset depicts the correlation length of the spin stripes $\xi_s = 2\pi/\Delta q$, where Δq is the full width at half maximum of the Lorentzian fit to the peak in S_s . (c,d) Similar data for systems with $t' = -0.25$ and $t' = 0.25$, respectively. The slopes of the dashed lines are $5/8$ and $5/4$.

pendence $\epsilon_s = \delta/2$ and $\epsilon_c = \delta$ as in the four-leg bilayer. However, in the square systems the linear dependence does not change across the transition from the region where the correlation length of the spin stripes, ξ_s , exceeds the system size to the regime where $\xi_s < L$. Fig. 4c demonstrates that changing the hopping amplitude to $t' = -0.25$ has little effect on the doping range that supports stripes and on the stripes correlation length. At the same time, the slope of $\epsilon_c(\delta)$ increases, thereby implying that the number of holes per unit length of a charge stripe reduces from 1 for $t' = 0$ to $2/3$ - $4/5$ when $t' = -0.25$. This observation bears resemblance to the findings of a recent DMRG study of a six-leg Hubbard cylinder [14]. Finally, the square $t' = 0.25$ systems show signatures of fractionally filled charge stripes that we did not detect in the four-leg torus. Furthermore, spin stripes appear at lower doping levels in the square systems than in the four-leg bilayer, see Fig. 4d. In fact, given the limited

range of system sizes available to us, we are unable to exclude the existence of spin stripes at even lower values of δ as L is further increased.

C. Superconductivity

The question of whether the two-dimensional repulsive Hubbard model exhibits superconductivity at a temperature scale that is relevant to the cuprate superconductors has been the focus of extensive research over the years. The current evidence points to a negative answer when $t' = 0$ [12], and arguably also for $t' < 0$ [14]. The situation is somewhat more promising for $t' > 0$, where power-law d -SC correlations are detected, albeit with a faster decay than the CDW correlations [14]. Hence, it is interesting to look for signs of superconductivity in the bilayer model, with emphasis on d -SC, which is expected

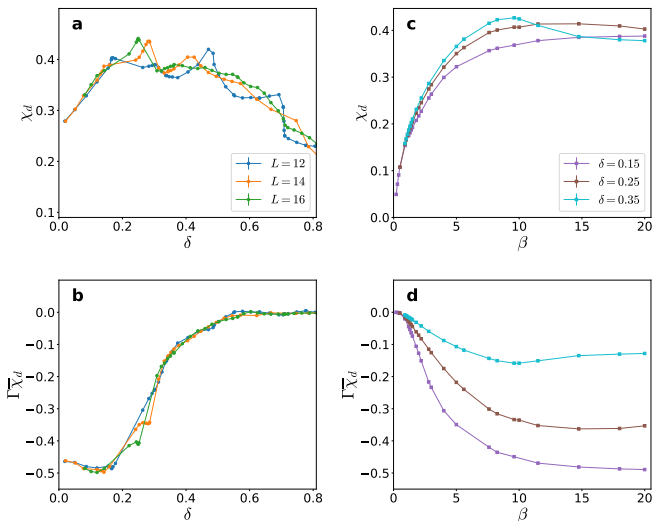


FIG. 5. (a) The intra-layer d -wave pairing susceptibility as a function of hole doping for $L \times L$ periodic systems with $t' = 0$ at $T = 0.05$. (b) The d -wave superconducting vertex times the uncorrelated pairing susceptibility of the same systems. (c,d) The same quantities as a function of inverse temperature β for an $L = 14$ bilayer at the specified hole doping levels.

to be the dominant channel in the presence of repulsive interactions.

To this end, we have calculated the intra-layer d -wave pair-field susceptibility

$$\chi_d = \frac{1}{2} \int_0^\beta d\tau \sum_{l=1,2} \sum_i \langle \Delta_d(l, \mathbf{r}_i, \tau) \Delta_d^\dagger(l, \mathbf{0}, 0) \rangle, \quad (5)$$

where $\Delta_d(l, \mathbf{r}_i) = \frac{1}{4} \sum_{\alpha=\pm\hat{x}, \pm\hat{y}} \eta_\alpha (c_{li\uparrow} c_{li+\alpha\downarrow} - c_{li\downarrow} c_{li+\alpha\uparrow})$ with $\eta_\alpha = 1$ for $\alpha = \pm\hat{x}$ and $\eta_\alpha = -1$ for $\alpha = \pm\hat{y}$. To reveal the effects of interactions on the superconducting properties we have also evaluated the particle-particle interaction vertex

$$\Gamma = \frac{1}{\chi_d} - \frac{1}{\bar{\chi}_d}, \quad (6)$$

where $\bar{\chi}_d$ is the uncorrelated d -wave pair-field susceptibility [36]. Onset of superconducting quasi-long-range order in the two-dimensional thermodynamic limit manifests itself by an increase of χ_d with decreasing temperature. In a finite system of linear size L the temperature dependence should also exhibit BKT finite-size scaling of the form $\chi_d = L^{7/4} f(L/\xi)$, where ξ is the BKT correlation length, see e.g. Refs. [37, 38]. In particular, one expects χ_d to saturate at low temperatures at a value that increases with L . Concomitantly, if the interactions indeed drive the system towards a superconducting instability then the product $\Gamma\bar{\chi}_d$ should approach -1 at the critical temperature.

We find none of the above signatures in the data for $t' = 0$ bilayers, as presented in Fig. 5. In particular, it is clear that both χ_d and $\Gamma\bar{\chi}_d$ are already saturated at

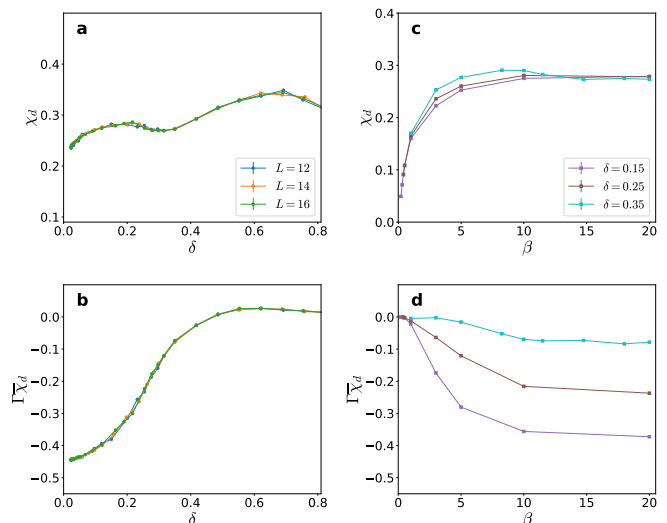


FIG. 6. Same as Fig. 5 but for $t' = -0.25$

the lowest temperature, $T = 0.05$, that we have considered. However, both quantities show no significant size dependence at this temperature, with χ_d exhibiting some fluctuations as a function of δ , which we attribute to finite size effects. Furthermore, while χ_d reaches a maximum around $\delta = 0.25$, $\Gamma\bar{\chi}_d$ attains its minimal value of about -0.5 near $\delta = 0.1$. The lack of correlation between the doping dependence of the two functions is further evidence that the $t' = 0$ bilayer shows no signs of a d -SC instability. Fig. 6 shows that a similar behavior is found for $t' = -0.25$. If at all, the indications for d -SC are weaker, in the sense that χ_d is maximal at $\delta = 0.7$ whereas the minimum of $\Gamma\bar{\chi}_d$ occurs near half filling and is slightly higher than its $t' = 0$ value. These findings conform well with the results of a DQMC study of a $t' = -0.25$ single Hubbard layer, albeit at higher temperatures [26]. Finally, the systems with $t' = 0.25$ exhibit the most favorable hints for the existence of some d -SC tendencies. Specifically, χ_d and $\Gamma\bar{\chi}_d$ show simultaneous maximal response at low doping levels below $\delta = 0.2$, that is also the largest among the bilayers that we have studied, see Fig. 7. Nevertheless, the fact that the response is still far from the instability threshold and does not show the expected finite-size scaling leads us to conclude that d -SC does not materialize in the bilayer model, at least for the parameters used by us.

One may object to the sweeping nature of the last statement as we have only referred to signs of uniform d -SC order. Indeed, there have been suggestions that the cuprate superconductors and perhaps some theoretical models may harbor the more elusive pair-density wave (PDW) state that is associated with a spatially oscillating superconducting order parameter of zero mean [39]. On the theoretical side, the stabilization of a PDW in interacting fermionic models has been proved difficult, with the best evidence for PDW correlations emerging from DMRG studies of a one-dimensional Kondo-Heisenberg

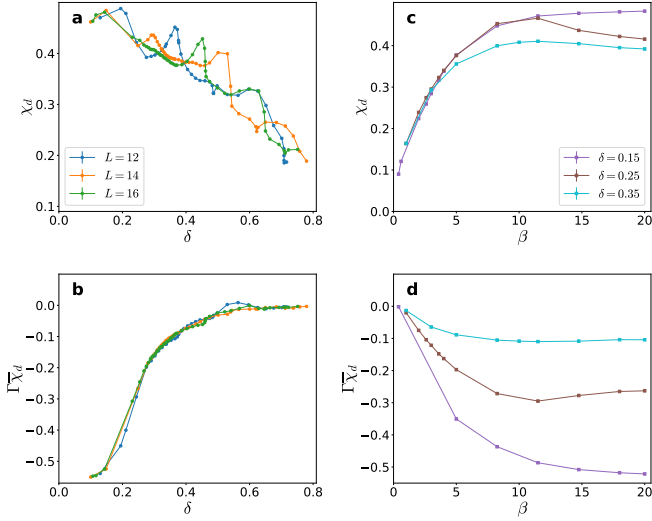


FIG. 7. Same as Fig. 5 but for $t' = 0.25$

chain [40] and of the strong-coupling limit of a Holstein-Hubbard cylinder [41]. To address the possibility of the existence of d -wave pairing with a non-zero center-of-mass momentum we have calculated the Fourier transform of the pair-field susceptibility in Eq. (5). However, our results show a single and robust peak of $\chi_d(\mathbf{q})$ at $\mathbf{q} = 0$ with no evidence for a PDW.

Despite not finding a pairing instability in the intra-layer d -wave channel we have not exhausted the search for superconductivity. Indeed, a more universal indicator of superconductivity is the superfluid stiffness, calculated from the response to a vector potential that couples identically to the two layers via [42]

$$\rho_s = \frac{1}{4} [\Lambda_{xx}(q_x \rightarrow 0, q_y = 0) - \Lambda_{xx}(q_x = 0, q_y \rightarrow 0)], \quad (7)$$

where

$$\Lambda_{xx}(\mathbf{q}) = \frac{1}{2L^2} \sum_{l,l'=1,2} \int_0^\beta d\tau \langle j_x(\mathbf{q}, l, \tau) j_x(-\mathbf{q}, l', 0) \rangle. \quad (8)$$

Here, $j_x(\mathbf{q}, l) = -i \sum_{j,\sigma} \{ c_{l,j,\sigma}^\dagger [t c_{l,j+\hat{x},\sigma} + t'(c_{l,j+\hat{x}+\hat{y},\sigma} + c_{l,j+\hat{x}-\hat{y},\sigma})] - \text{H.c.} \} e^{-i\mathbf{q}\cdot\mathbf{r}_j}$, is the Fourier transform of the current density operator in the x direction. In the finite $L \times L$ bilayers that we simulate we obtain the limit $q \rightarrow 0$ in Eq. (7) by extrapolating Λ_{xx} using its values at $q = 2\pi/L$ and $q = 4\pi/L$. A typical temperature dependence of ρ_s is depicted in Fig. 8d for $t' = 0$ systems at $\delta = 0.35$. Clearly, ρ_s at this doping level shows little size dependence and obeys the criterion for the BKT transition $\rho_s(T_{BKT}) = (2/\pi)T_{BKT}$ at a critical temperature $T_{BKT} \simeq 0.08$. Fig. 8b shows that the bilayer undergoes a BKT transition to a superconducting state over an extended range of hole doping. The figure depicts the ratio $\rho_s(T)/(2T/\pi)$ at $T = 0.05$, such that any point for which the ratio is larger than one corresponds to a system that

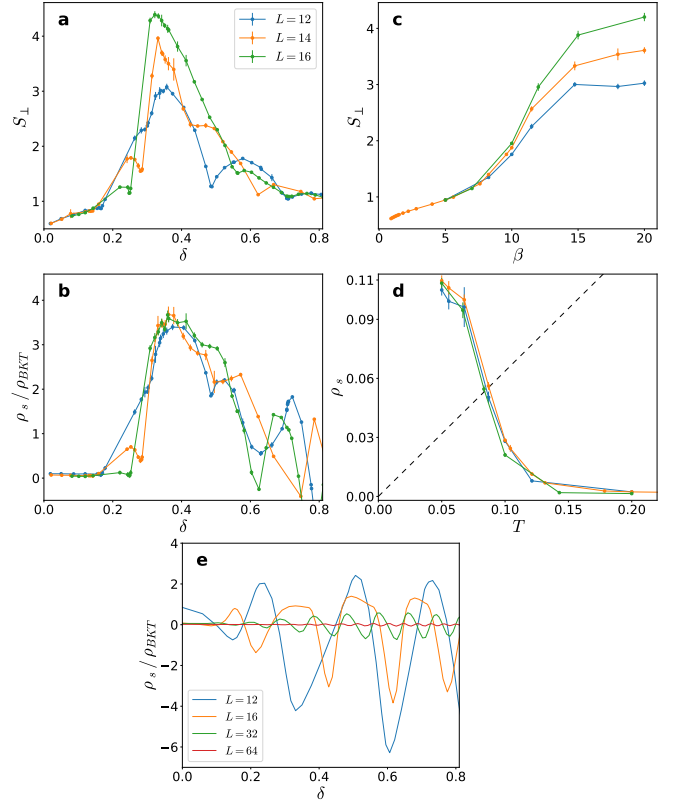


FIG. 8. (a) The equal-time inter-layer pair correlations as a function of doping for $L \times L$ periodic systems with $t' = 0$ at $T = 0.05$. (b) The superfluid stiffness of the systems, normalized by $\rho_{BKT} = 2T/\pi = 0.1/\pi$. (c,d) The pair correlations and the superfluid stiffness as a function of temperature for $\delta = 0.35$. The dashed line depicts $2T/\pi$. (e) The superfluid stiffness of non-interacting ($U=0$) bilayers at $T = 0.05$.

exhibits a transition at a temperature $T > 0.05$. The results also demonstrate the strong finite-size effects in ρ_s at high doping levels, which cause the stiffness to oscillate between positive and negative values. Such a behavior reflects changes in the Fermi surface and is inherited from the non-interacting limit, see Fig. 8e. It is noticeable whenever the interaction effects are diminished, as is the case for large δ . This issue can be mitigated by introducing a weak uniform magnetic field to the model [43], but we forewent the modification since the problem is significant only in a region where the qualitative behavior is already clear.

A question remains as to the nature of the superconducting state. The presence of the ferromagnetic interaction between the layers makes inter-layer spin polarized pairing a natural candidate for the instability channel. We have corroborated this hypothesis by calculating the equal-time inter-layer pair correlations

$$S_\perp = \frac{1}{2} \sum_{i\sigma} \langle \Delta_{\perp\sigma}(\mathbf{r}_i) \Delta_{\perp\sigma}^\dagger(\mathbf{0}) \rangle, \quad (9)$$

where $\Delta_{\perp\sigma}(\mathbf{r}_i) = c_{1i\sigma} c_{2i\sigma}$. Fig. 8c shows that the tem-

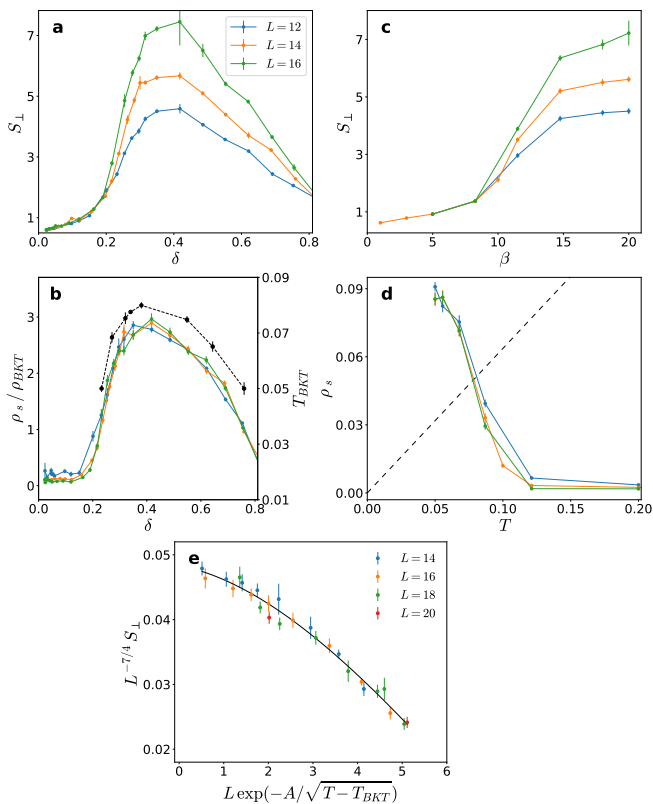


FIG. 9. Same as Figure 8 but for $t' = -0.25$. The black curve in (b) depicts the BKT transition temperature, deduced from the BKT criterion, as a function of doping. Panel (e) depicts the collapse of the S_{\perp} data for a system with $\delta = 0.35$ using the expected BKT scaling. The line is a guide to the eye.

perature dependence of S_{\perp} begins to develop size dependence slightly above T_{BKT} and saturates at low temperatures to a value that grows with L . These signatures strongly support the identification of T_{BKT} with the onset of quasi-long-range Δ_{\perp} correlations. Furthermore, the doping dependence of the low-temperature S_{\perp} follows that of ρ_s and exhibits size dependence within the range of doping levels where the system is below its T_{BKT} according to the BKT criterion, see Fig. 8a. We note that S_{\perp} of the $t' = 0$ bilayers attains its maximum around $\delta = 0.35$. This fact may be tied to the decline of the intra-layer d -SC susceptibility of the $\delta = 0.35$ system at temperatures below its T_{BKT} , as seen in Fig. 5c.

Both ρ_s and S_{\perp} continue to exhibit similar trends in the presence of non-zero t' . Fig. 9 shows that the $t' = -0.25$ bilayer sustains a superconducting phase over a wider range of doping levels as compared to the $t' = 0$ bilayer. The figure also contains results for the doping dependence of T_{BKT} , as deduced from the BKT criterion, and demonstrates that it follows the behavior of the low-temperature superfluid stiffness. Namely, the two trace a dome as a function of δ , achieving a maximum around $\delta = 0.4$. Further evidence in favor of the onset of quasi-long range order comes from apply-

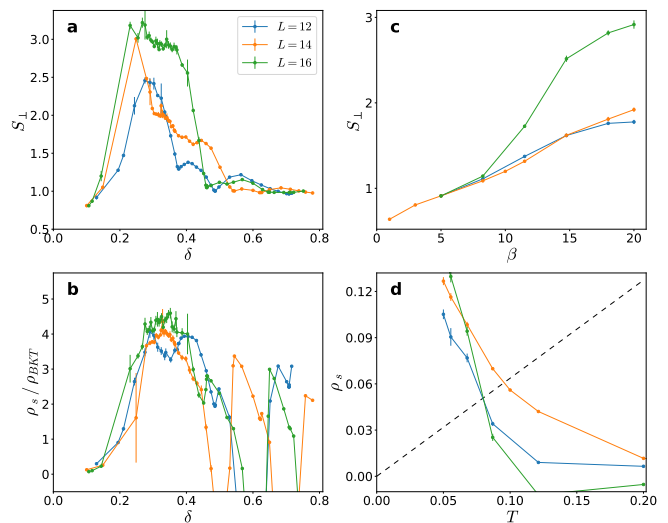


FIG. 10. Same as Figure 8 but for $t' = 0.25$

ing the BKT scaling ansatz $S_{\perp}(L, T) = L^{7/4} f[L/\xi(T)]$, where $\xi(T) \sim \exp[A/(T - T_{BKT})^{1/2}]$, as $T \rightarrow T_{BKT}$ from above. Fig. 9(e) shows the scaling, where $A = 0.17$ and $T_{BKT} = 0.72$ yield the best data collapse. Fig. 10 shows that for $t' = 0.25$ the leading edge of the superconducting dome shifts to lower values of doping, somewhat below $\delta = 0.2$. For reasons that are not clear to us the fluctuations associated with finite size effects are much reduced in the results for the $t' = -0.25$ bilayers, while they are enhanced in the $t' = 0.25$ systems.

We end this section by considering possible correlations between the superconducting properties of the model and its uniform magnetic susceptibility along the z direction (the Knight shift). The temperature dependence of the Knight shift is presented in Fig. 11 for a $t' = 0$ system at several doping levels. We find that it exhibits a peak at a temperature T^* that reduces with increasing hole doping until $\delta \approx 0.3$, where it levels off. In the context of the cuprates such a peak is used to define a crossover scale that is associated with the opening of a pseudogap. As far as the model is concerned, there seems to be no clear correspondence between T^* and the behavior of the d -SC signatures. From Fig. 5 it is evident that the low temperature $\Gamma\chi_d$ does not change within the range of doping levels in which T^* changes by more than a factor of 3, while χ_d increases over the same range. Both quantities appear to saturate at a similar temperature that shows no considerable dependence on doping, and hence on T^* . On the other hand, the inter-layer superconductivity onsets at a doping level which coincides with the point where T^* becomes δ -independent, see Figs. 8 and 11. However, the causal relation between the two phenomena is unclear. Regardless of its relevance to superconductivity, the appearance of the peak and the general behaviour of T^* are in agreement with DQMC results obtained for the Hubbard model at more elevated temperatures [26]. This fact reinforces the conclusion that despite the difference

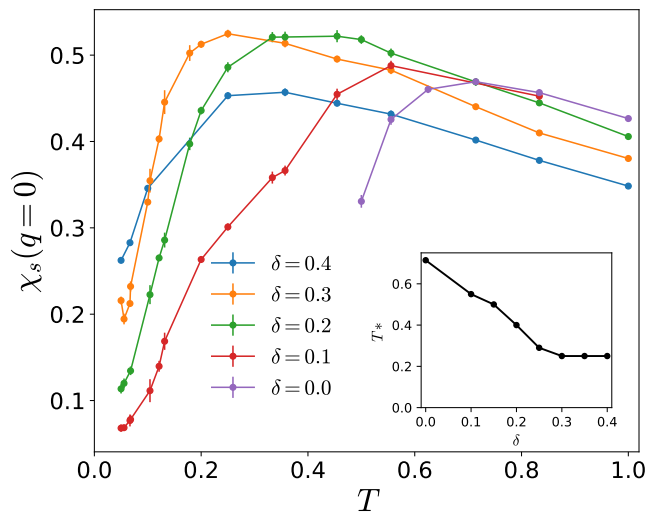


FIG. 11. The $q = 0$ spin susceptibility (Knight shift) versus temperature for various doping levels of the 14×14 $t' = 0$ system. The curves display a maximum at a temperature denoted by T^* . The inset depicts T^* as a function of doping.

in their symmetries the bilayer model and the Hubbard model display many common physical properties.

IV. SUMMARY AND OUTLOOK

What are the low-temperature properties of the repulsive two-dimensional Hubbard model at the intermediate coupling regime $U \sim t$? By far, the most adopted approach towards answering this question has been to apply DMRG to $W \times L$ systems, then try to extract the $L \rightarrow \infty$ behavior for fixed W and finally look for W -independent characteristics within the limited range of computationally manageable widths. Less frequent attempts involved studying the model on a more two-dimensional geometry (typically square) using DQMC. However, this method suffers from the sign problem that constrains its application to relatively high temperatures, hence complicating the comparison with the DMRG results for the ground state. In the present work we have offered yet another route that applies sign-problem-free DQMC to a bilayer

model which contains the Hubbard interaction on each layer, at the expense of introducing a ferromagnetic attractive inter-layer coupling that breaks the global $SU(2)$ spin rotation symmetry. Our primary goal was to assess the degree by which the deformed model captures known behaviors of the Hubbard model or exhibits qualitatively new features.

We have found that in a similar fashion to DMRG and DQMC results for Hubbard systems, the most robust tendency of the bilayer model is to develop stripy modulations in its charge and spin densities. The agreement extends to specific properties of the observed stripe phases. Namely, the charge stripes are filled for $t' = 0$, exhibit fractional filling that is larger than $1/2$ when $t' = -0.25$, and are suppressed, especially at low doping levels, for $t' = 0.25$. The lack of spin rotation symmetry renders the z and x - y spin responses of the model inequivalent. Nevertheless, the z component of the spin density shows very clear stripes, which become short-range correlated and appear without accompanying charge stripes at high doping. Whenever spin and charge stripes coexist the period of the first is approximately twice that of the second.

Intra-layer d -SC is absent in the bilayer model, at least for the parameters that we have considered and down to a temperature of $T = 0.05$ (which appears to be sufficiently low to allow extending this conclusion to the ground state). In accord with DMRG studies of Hubbard cylinders, systems with $t' > 0$ show stronger signatures of d -SC. However, none of them come close to the required level for a superconducting instability. In contrast, we detect clear signs of inter-layer spin-polarized superconductivity, which is expected in light of the attractive ferromagnetic interaction that exists in the model.

Overall, our findings demonstrate that the bilayer model constitutes a valuable computational proxy to the Hubbard model, and may serve as a controlled test bed to study further aspects of strongly correlated electrons. To this end, one may consider augmenting the bilayer Hamiltonian with additional terms, which nevertheless preserve the symmetry that keeps it free from the sign problem. This strategy may also be pursued in order to suppress the inter-layer superconductivity since it can act as a masking agent that obscures evidence for more interesting forms of superconductivity at low temperatures.

[1] D. P. Arovas, E. Berg, S. A. Kivelson, and S. Raghu, "The Hubbard model", *Annu. Rev. Condens. Matter Phys.* **13**, 239 (2022).
 [2] C. N. Varney, C.-R. Lee, Z. J. Bai, S. Chiesa, M. Jarrell, and R. T. Scalettar, "Quantum Monte Carlo study of the two-dimensional fermion Hubbard model", *Phys. Rev. B* **80**, 075116 (2009).
 [3] S. Raghu, S. A. Kivelson, and D. J. Scalapino, "Superconductivity in the repulsive Hubbard model: An asymptotically exact weak-coupling solution", *Phys. Rev. B* **81**,

224505 (2010).
 [4] Y. Nagaoka, "Ferromagnetism in a narrow, almost half-filled s band", *Phys. Rev.* **147**, 392 (1966).
 [5] S. R. White and D. J. Scalapino, "Stripes on a 6-leg Hubbard ladder", *Phys. Rev. Lett.* **91**, 136403 (2003).
 [6] G. Hager, G. Wellein, E. Jeckelmann, and H. Fehske, "Stripe formation in doped Hubbard ladders", *Phys. Rev. B* **71**, 075108 (2005).
 [7] G. Ehlers, S. R. White, and R. M. Noack, "Hybrid-space density matrix renormalization group study of the

- doped two-dimensional Hubbard model”, Phys. Rev. B **95**, 125125 (2017).
- [8] B.-X. Zheng, C.-M. Chung, P. Corboz, G. Ehlers, M.-P. Qin, R. M. Noack, H. Shi, S. R. White, S. Zhang, and G. K.-L. Chan, ”Stripe order in the underdoped region of the two-dimensional Hubbard model”, Science **358**, 1155 (2017).
- [9] H.-C. Jiang and T. P. Devereaux, ”Superconductivity in the doped Hubbard model and its interplay with next-nearest hopping t'' ”, Science **365**, 1424 (2019).
- [10] C.-M. Chung, M. Qin, S. Zhang, U. Schollwöck, and S. R. White, ”Plaquette versus ordinary d -wave pairing in the t' -Hubbard model on a width-4 cylinder”, Phys. Rev. B **102**, 041106(R) (2020).
- [11] Y.-F. Jiang, J. Zaanen, T. P. Devereaux, and H.-C. Jiang, ”Ground state phase diagram of the doped Hubbard model on the four-leg cylinder”, Phys. Rev. Res. **2**, 033073 (2020).
- [12] M. Qin, C.-M. Chung, H. Shi, E. Vitali, C. Hubig, U. Schollwöck, S. R. White, and S. Zhang, ”Absence of superconductivity in the pure two-dimensional Hubbard model”, Phys. Rev. X **10**, 031016 (2020).
- [13] H. Xu, C.-M. Chung, M. Qin, U. Schollwöck, S. R. White, and S. Zhang, ”Coexistence of superconductivity with partially filled stripes in the Hubbard model”, arXiv:2303.08376.
- [14] Y.F. Jiang, T. P. Devereaux, and H.-C. Jiang, ”Ground state phase diagram and superconductivity of the doped Hubbard model on six-leg square cylinders”, arXiv:2303.15541.
- [15] S. R. White and D. J. Scalapino, ”Competition between stripes and pairing in a t - t' - J model”, Phys. Rev. B **60**, R753 (1999).
- [16] S. R. White and D. J. Scalapino, ”Pairing on striped t - t' - J lattices”, Phys. Rev. B **79**, 220504(R) (2009).
- [17] S. R. White and D. J. Scalapino, ”Stripe structures in the t - t' - J model”, Physica C **481**, 146 (2012).
- [18] J. F. Dodaro, H.-C. Jiang, and S. A. Kivelson, ”Intertwined order in a frustrated four-leg t - J cylinder”, Phys. Rev. B **95**, 155116 (2017).
- [19] H.-C. Jiang, Z.-Y. Weng, and S. A. Kivelson, ”Superconductivity in the doped t - J model: Results for four-leg cylinders”, Phys. Rev. B **98**, 140505(R) (2018).
- [20] H.-C. Jiang and S. A. Kivelson, ”High temperature superconductivity in a lightly doped quantum spin liquid”, Phys. Rev. Lett. **127**, 097002 (2021).
- [21] S. Gong, W. Zhu, and D. N. Sheng, ”Robust d -Wave superconductivity in the square-lattice t - J model”, Phys. Rev. Lett. **127**, 097003 (2021).
- [22] S. Jiang, D. J. Scalapino, and S. R. White, ”Ground-state phase diagram of the t - t' - J model”, Proc. Natl. Acad. Sci. **118**, e2109978118 (2021).
- [23] X. Lu, F. Chen, W. Zhu, D. N. Sheng, and S.-S. Gong, ”Emergent superconductivity and competing charge orders in hole-doped square-lattice t - J model”, arXiv:2304.03963.
- [24] E. W. Huang, C. B. Mendl, S. Liu, S. Johnston, H.-C. Jiang, B. Moritz, and T. P. Devereaux, ”Numerical evidence of fluctuating stripes in the normal state of high- T_c cuprate superconductors”, Science **358**, 1161 (2017).
- [25] E. W. Huang, C. B. Mendl, H.-C. Jiang, B. Moritz, and T. P. Devereaux, ”Stripe order from the perspective of the Hubbard model”, npj Quantum Mater. **3**, 22 (2018).
- [26] E. W. Huang, W. O. Wang, J. K. Ding, T. Liu, F. Liu, X.-X. Huang, B. Moritz, and T. P. Devereaux, ”Intertwined states at finite temperatures in the Hubbard model”, J. Phys. Soc. Jpn. **90**, 111010 (2021).
- [27] S. Yang, T. Ying, W. Li, J. Yang, X. Sun, and X. Li, ”Quantum Monte Carlo study of the Hubbard model with next-nearest-neighbor hopping t' : pairing and magnetism”, J. Phys.: Condens. Matter **33**, 115601 (2021).
- [28] F. F. Assaad, V. Rousseau, F. Hebert, M. Feldbacher, and G. G. Batrouni, ”Spin and charge dynamics of stripes in doped Mott insulators”, Europhys Lett. **63**, 569 (2003).
- [29] C. Wu and S.-C. Zhang, ”Sufficient condition for absence of the sign problem in the fermionic quantum Monte Carlo algorithm”, Phys. Rev. B **71**, 155115 (2005).
- [30] F. F. Assaad, M. Imada and D. J. Scalapino, ”Charge and spin structures of a $d_{x^2-y^2}$ superconductor in the proximity of an antiferromagnetic Mott insulator”, Phys. Rev. B **56**, 15001 (1997).
- [31] See Supplemental Material for additional details on the sensitivity of the results to the value of $\Delta\tau$ and for the dependence of the hole concentration on the chemical potential. Also included are representative examples of the spin susceptibility along different directions, and results for the pairing susceptibility and the superconducting vertex in the inter-layer pairing channel.
- [32] A. Moreo, D. Scalapino, and E. Dagotto, ”Phase separation in the Hubbard model”, Phys. Rev. B **43**, 11442 (1991).
- [33] A. Macridin, M. Jarrell, and T. Maier, ”Phase separation in the Hubbard model using the dynamical cluster approximation”, Phys. Rev. B **74**, 085104 (2006).
- [34] K. Fang, G. W. Fernando, A. V. Balatsky, and A. N. Kocharian, ”Possible phase separation in square and honeycomb Hubbard model: A variational cluster study”, Phys. Lett. A **379**, 2230 (2015).
- [35] No background is added when fitting S_s . On purely phenomenological basis we use a background of the form $\sqrt{|q_x/2\pi|}$ when fitting S_c . The position, width and height of the Lorentzians, as well as the background amplitude, are obtained by a standard least squares fit.
- [36] S. R. White, D. J. Scalapino, R. L. Sugar, N. E. Bickers, and R. T. Scalettar, ”Attractive and repulsive pairing interaction vertices for the two-dimensional Hubbard model”, Phys. Rev. B **39**, 839 (1989).
- [37] N. C. Costa, T. Blommel, W.-T. Chiu, G. Batrouni, and R. T. Scalettar, ”Phonon dispersion and the competition between pairing and charge order”, Phys. Rev. Lett. **120**, 187003 (2018).
- [38] R. A. Fontenele, N. C. Costa, R. R. dos Santos, and T. Paiva, ”Two-dimensional attractive Hubbard model and the BCS-BEC crossover”, Phys. Rev. B **108**, 184502 (2022).
- [39] D. F. Agterberg, J. C. S. Davis, S. D. Edkins, E. Fradkin, D. J. Van Harlingen, S. A. Kivelson, P. A. Lee, L. Radzihovsky, J. M. Tranquada, and Y. Wang, ”The physics of pair-density waves: Cuprate superconductors and beyond”, Annu. Rev. Condens. Matter Phys. **11**, 231 (2020).
- [40] E. Berg, E. Fradkin, and S. A. Kivelson, ”Pair-density wave correlations in the Kondo-Heisenberg model”, Phys. Rev. Lett. **105**, 146403 (2010).
- [41] K. S. Huang, Z. Han, S. A. Kivelson, and H. Yao, ”Pair-density-wave in the strong coupling limit of the Holstein-Hubbard model”, npj Quantum Mater. **7**, 17 (2022).

- [42] D. J. Scalapino, S. R. White, and S. Zhang, "Insulator, metal, or superconductor: The criteria", Phys. Rev. B **47**, 7995 (1993).
- [43] F. F. Assaad, "Depleted Kondo lattices: Quantum Monte Carlo and mean-field calculations", Phys. Rev. B **65**, 115104 (2002).

Supplemental Material for: "Quantum Monte Carlo study of a bilayer $U(2) \times U(2)$ symmetric Hubbard model"

Yosef Caplan¹ and Dror Orgad¹

¹*Racah Institute of Physics, The Hebrew University, Jerusalem 91904, Israel*

A. Sensitivity of the results to the value of $\Delta\tau$

Fig. 1 depicts representative examples of the dependence of the electronic density and of the spin structure factor on the value of the Trotter step size $\Delta\tau$. The figure demonstrates that decreasing $\Delta\tau$ beyond 0.1 (the value used by us throughout the calculations) leads to a change of less than 1% in $\langle n \rangle$ and less than 5% in S_s .

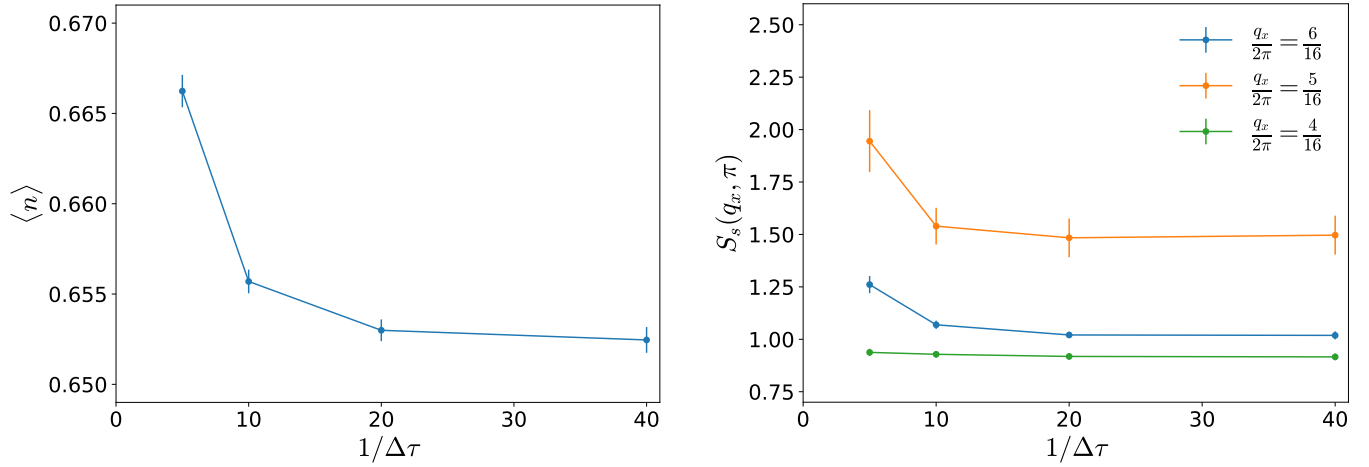


FIG. 1. Left: The dependence of the electronic density on $\Delta\tau$ in a system with $L = 16$, $t' = 0$ and $\beta = 20$. Right: The $\Delta\tau$ dependence of the z -spin structure factor at various values of q_x in the same system with $\mu = -1.7$.

B. Dependence of the electronic density on the chemical potential

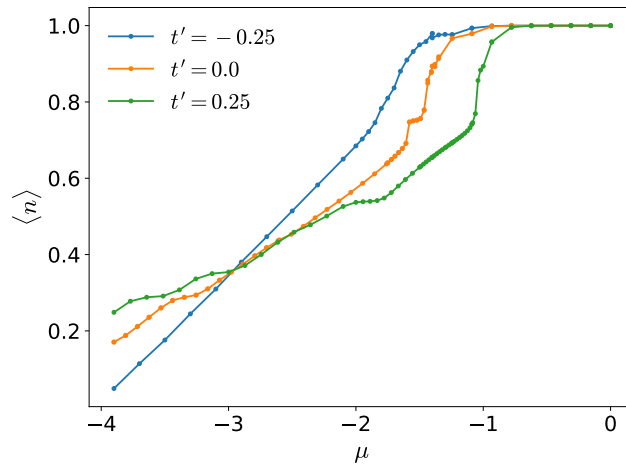


FIG. 2. The dependence of the electronic density on the chemical potential for $L = 16$ systems at $\beta = 20$.

C. Examples of the spin susceptibility along the z and transverse directions

To make the consequences of breaking the spin-SU(2) symmetry apparent we include examples of the spin susceptibility

$$\chi_s^\mu(\mathbf{q}) = 2 \int_0^\beta d\tau \sum_{l,i} e^{-i\mathbf{q}\cdot\mathbf{r}_i} \langle S^\mu(l, \mathbf{r}_i, \tau) S^\mu(l, \mathbf{0}, 0) \rangle, \quad (1)$$

along different directions. Here $S^\mu(l, \mathbf{r}_i) = \frac{1}{2} \sum_{\alpha, \beta = \uparrow, \downarrow} c_{l, \mathbf{r}_i, \alpha}^\dagger \sigma_{\alpha\beta}^\mu c_{l, \mathbf{r}_i, \beta}$, with σ the Pauli matrices.

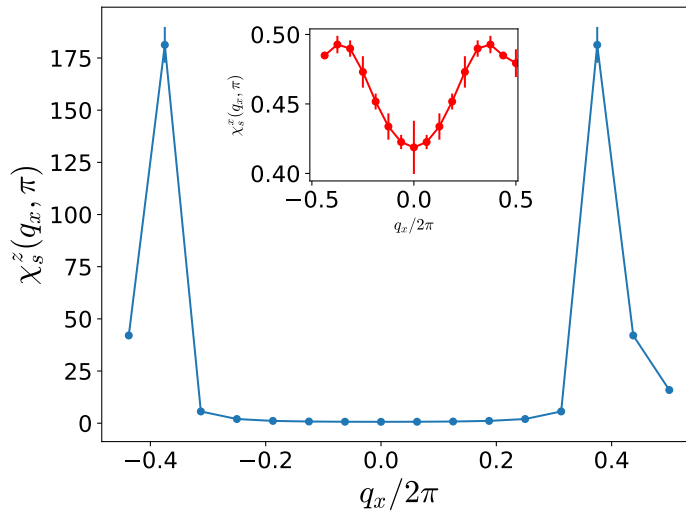


FIG. 3. The spin susceptibility in the z and x directions for a $L = 16$, $t' = -0.25$ system at $\beta = 20$ and $\delta = 0.165$.

D. The inter-layer pairing susceptibility and the corresponding vertex

Here we show results for the inter-layer pairing susceptibility

$$\chi_{\perp} = \frac{1}{2} \int_0^{\beta} d\tau \sum_{i,\sigma} \langle \Delta_{\perp\sigma}(\mathbf{r}_i, \tau) \Delta_{\perp\sigma}^{\dagger}(\mathbf{0}, 0) \rangle, \quad (2)$$

and for $\Gamma_{\perp} \bar{\chi}_{\perp}$, where the inter-layer pairing vertex is defined via χ_{\perp} and the uncorrelated inter-layer pair-field susceptibility $\bar{\chi}_{\perp}$ according to

$$\Gamma_{\perp} = \frac{1}{\chi_{\perp}} - \frac{1}{\bar{\chi}_{\perp}}. \quad (3)$$

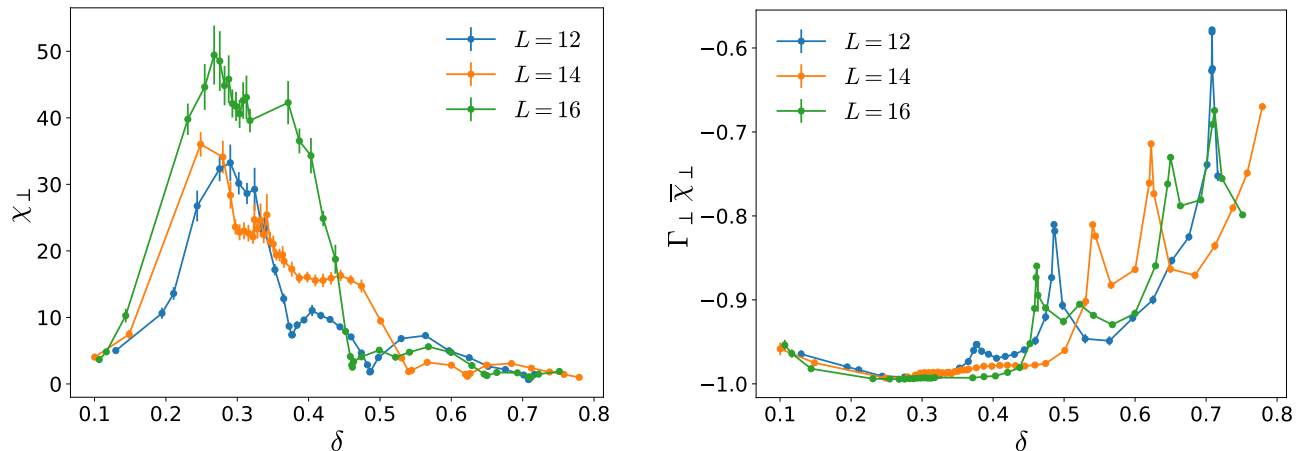


FIG. 4. Left: The inter-layer pairing susceptibility as a function of hole doping for square periodic systems with $t' = 0.25$ at $\beta = 20$. Right: $\Gamma_{\perp} \bar{\chi}_{\perp}$ for the same systems.